Surface-Enhanced Raman Spectra of Aza-aromatics on Nanocrystals of Metallic ReO_3

Kanishka Biswas,[†,‡] S. V. Bhat,[†] and C. N. R. Rao*[,†,‡]

Chemistry and Physics of Materials Unit, DST Unit on Nanoscience and CSIR Centre of Excellence in Chemistry, Jawaharlal Nehru Centre for Advanced Scientific Research Jakkur P. O., Bangalore 560064, India, and Solid State and Structural Chemistry Unit, Indian Institute of Science, Bangalore 560012, India

Received: December 22, 2006; In Final Form: February 8, 2007

Surface-enhanced Raman spectra (SERS) of pyridine have been investigated on the surfaces of the metallic ReO_3 nanocrystals with diameters in the range of 12−32.5 nm. On ReO_3 nanocrystal surfaces, the Raman bands of pyridine generally shift toward lower frequencies, accompanied by enhancement of intensity. The frequency shift does not vary with particle size, but band intensification is highest with the 17 nm nanocrystals. The study establishes how an oxide metal can be employed equally effectively to observe SERS of molecules. On the basis of the success with the study of pyridine, we have extended the study to SERS of pyrimidine and pyrazine on 17 nm ReO_3 nanocrystals. The SERS effect observed in the three aza-aromatics demonstrates the presence of bonding interaction between the ReO_3 surface and the adsorbed molecules.

Introduction

Surface-enhanced Raman spectroscopy has emerged as an important spectroscopic method for surface science, analytical chemistry, physical chemistry, and biophysics because of the enhanced vibrational signals, low detection limits, and good adsorbate selectivity. The magnitude of surface enhancement is affected by factors such as surface roughness, particle size and shape, the nature of the analyte, and wavelength of laser excitation.[1−6] The major contributions to surface-enhanced Raman spectra (SERS) effect are due to the electromagnetic (EM) enhancement associated with large local fields caused by surface plasmon resonance, and chemical enhancement involving a resonance Raman-like process associated with chemical interactions between the molecule and the metal surface. EM enhancement is determined by the interaction of the incident and scattered light and the metal, which depends on the wavelength of the exciting light, the optical electronic property of metal, and surface morphology. Chemical enhancement is determined by chemisorption and the charge-transfer between the adsorbate and the substrate. In most noble metals, EM enhancement plays a dominant role. Since the early measurement of the surface-enhanced Raman spectrum of pyridine adsorbed on an electrochemically roughened Ag electrode by Fleischmann et al.,[7] there has been a wide range of studies on Ag,[7−15] Au[8,9,16−19] and other metals such as Pt, Ru, Rh, Pd, Fe, Co, and Ni.[20−24] A comparative SERS study of pyridine with different metals has been carried out.[25] In most cases, the enhancement factor is in the range of 10^2-10^7. Large enhancement factors on the order of $10^{14}-10^{15}$ as well as single-molecule SERS have been reported for molecules at the junctions between nanoparticles.[26−29] We have investigated SERS of pyridine on ReO_3 nanocrystals, since ReO_3 is a unique oxide metal which looks like copper and conducts like copper.[30] ReO_3 shows a plasmon band like gold around 520 nm in the visible region. Nanocrystals of ReO_3 of different sizes exhibit a size dependence of the plasmon band position.[31] We have examined the SERS of pyridine on ReO_3 nanocrystals of different sizes and obtained the relative enhancement ratios of the adsorbate bands relative to those of the pure liquid.[8,12] We have found that the values of the relative enhancement ratios on the ReO_3 surface to be comparable to those reported in the literature in the case of nobel metal particles. The enhancement factors are of the order of 10^5-10^6. The bands of the pyridine adsorbed on the ReO_3 nanocrystals are shifted significantly toward lower frequencies due to bonding between the ReO_3 surface and the molecule lying on the surface. SERS effect on ReO_3 nanocrystals is also found with pyrimidine and pyrazine, thereby establishing the oxide metal to be as effective as Au or Ag nanoparticles.

Experimental Section

ReO_3 nanocrystals in the diameter range of 12−32.5 nm were prepared by the decomposition of the Re_2O_7−dioxane complex under solvothermal conditions.[31] The synthesis of ReO_3 nanoparticles involves the preparation of the rhenium(VII) oxide−dioxane complex, $Re_2O_7-(C_4H_8O_2)_x$, as the starting material (following the literature procedure[32,33]) and its solvothermal decomposition in toluene to yield the desired nanoparticles. In a typical synthesis, 0.025 g (0.12 mmol) of Re_2O_7 was taken in a 10 mL round-bottomed flask and 0.25 mL (2.93 mmol) of anhydrous 1,4-dioxane was added to it. This mixture was warmed in a water bath maintained at 70 °C and then frozen in an ice bath alternatively until the rhenium(VII) oxide−dioxane complex (RDC) precipitated out as a dense, pearl gray deposit. The complex was dissolved in 2 mL (30.08 mmol) of ethanol and was taken in 45 mL of toluene and sealed in a Teflon-lined stainless steel autoclave of 80 mL capacity (at 70% filling fraction). It was then heated at 200 °C for 4 h. The red ReO_3 nanoparticles (12 nm diameter) were washed several times with acetone. To vary the particle size of ReO_3, the concentration of RDC and the reaction temperature were varied, keeping the amount of toluene and the filling fraction of the autoclave constant. Nanoparticles of different diameters were obtained as follows: for 12 nm, RDC dissolved in 2 mL (30.08 mmol)

* To whom correspondence should be addressed. Fax: +91 80 22082760. E-mail: cnrrao@jncasr.ac.in.
† Jawaharlal Nehru Centre for Advanced Scientific Research.
‡ Indian Institute of Science.

10.1021/jp068894i CCC: $37.00
Published on Web 03/24/2007

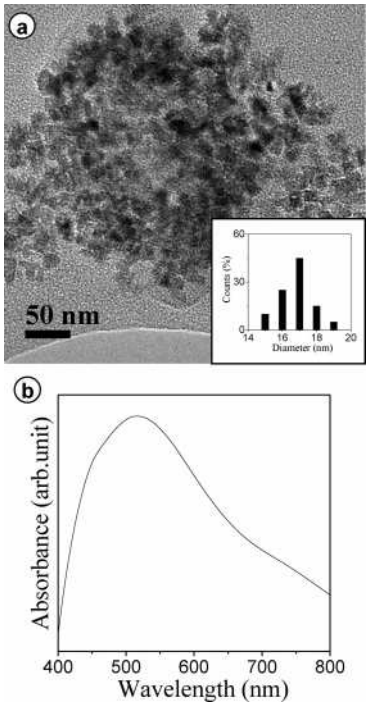

Figure 1. (a) TEM image of ReO_3 nanocrystals with an average diameter of 17 nm. Inset shows the size distribution histogram. (b) Absorption spectrum of 17 nm ReO_3 nanocrystals.

ethanol prepared by 0.025 g (0.12 mmol) of Re_2O_7 and 0.25 mL (2.93 mmol) of dioxane, 200 °C, 4 h; for 17 nm, RDC dissolved in 2 mL (30.08 mmol) ethanol prepared from 0.05 g (0.24 mmol) of Re_2O_7 and 0.5 mL (5.83 mmol) of dioxane, 200 °C, 4 h; for 32.5 nm, RDC dissolved in 2 mL (30.08 mmol) ethanol prepared from 0.05 g (0.24 mmol) of Re_2O_7 and 0.5 mL (5.83 mmol) of dioxane, 220 °C, 4 h.

For SERS measurements, we used the pure liquid or 10^{-3} M analyte (pyridine/pyrimidine/pyrazine) solution in milli-Q water. For each measurement, we took 3 mg of the ReO_3 nanocrystals on a clean glass slide in which 5 μL of the liquid anylate (pyridine/pyrimidine/pyrazine) was dropped. Raman spectroscopy was carried out with a LAB RAM HR 800 spectrometer. The excitation wavelength was 632.8 nm.

Results and Discussion

We have carried out SERS of pyridine on ReO_3 nanoparticles of three different sizes. The particles had average diameters of 12, 17, and 32.5 nm with plasmon band maxima at 507, 516, and 543 nm, respectively. The band maximum is not that different from that found in Au nanocrystals, but the band is broadly extended over the 400−700 nm regions. In Figure 1, we show the transmission electron microscope image and the surface plasmon band of the 17 nm nanocrystals to demonstrate the essential features. A first-order Raman spectrum is forbidden for ReO_3. It only shows second-order Raman scattering,[34] and we did not find any interference between Raman bands of the adsorbates and ReO_3.

Figure 2 shows the Raman spectra of pyridine on ReO_3 nanocrystals in the 600−1250 cm^{-1} region, along with the spectrum of the pure liquid. On adsorption of pyridine on the ReO_3 nanocrystals, we observe bands at 610 (ν_{6a}, A_1, asymmetric ring breathing), 632 (ν_{6b}, B_2, ring in plane deformation), 962 (ν_1, A_1, symmetric ring breathing), 1006 (ν_{12}, A_1, trigonal ring breathing), 1027 (ν_{18a}, A_1), and 1201 cm^{-1} (ν_{9a}, A_1, C−H in plane deformation), respectively.[25] In Table 1 we show the

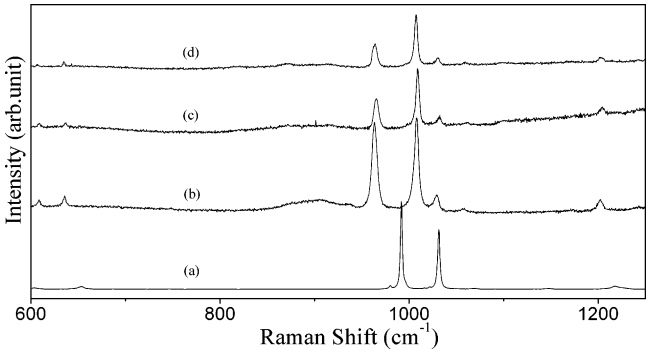

Figure 2. Raman spectra of pyridine: (a) in liquid state, (b) on 32.5 nm ReO_3, (c) on 17 nm ReO_3, and (d) on 12 nm ReO_3.

Raman band positions of pyridine on the ReO_3 nanocrystals along with their relative intensities in parentheses. The data for liquid pyridine are given for the purpose of comparison. From Table 1, we notice that the 610 cm^{-1} band of pyridine adsorbed on the ReO_3 nanocrystals does not show any significant change in the frequencies compared to pure pyridine, but the other five bands are shifted markedly toward lower frequencies, although all the bands show intensification. Only the band at 1582 cm^{-1} (ν_{8a}) due to ring stretching is shifted to higher frequency. The highest frequency shifts are found in the case of the 1068 (ν_{18a}), 991 (ν_1, symmetric ring breathing), and 1582 cm^{-1} ($\nu_{8a,}$ ring stretching) bands of pyridine, while the highest SERS intensification is found in the case of the shifted 1031 cm^{-1} (ν_{12}, trigonal ring breathing) band. The frequency of the ring breathing mode ν_1 is sensitive to weak σ donation and large σ/π back-donation. In the case of Au, Cu, and other transition metals, the ν_1 mode is shifted to higher frequencies, with the pyridine molecule adsorbed on the metal in the end-on configuration (binding by nitrogen lone pair).[16,25]

On the basis of the available data, we are not able to fully explain the frequency shifts of Raman bands of pyridine adsorbed on ReO_3 nanocrystals. We, however, suggest that the molecule could be in the flat-on configuration, or possibly making a small angle with respect to the surface. If the molecule lies flat on the metal surface, the ring breathing mode is expected to be lowered relative to that of the free pure molecule.[16] Such a behavior has been observed in the SERS of flat-adsorbed benzene on Ag.[35] The ring breathing mode of adsorbed benzene occurs at 982 cm^{-1}, compared to 992 cm^{-1} in liquid benzene.[35] In the present case, there is little doubt that there is significant bonding interaction between pyridine and the ReO_3 surface, but we are not able to decide on the symmetry of the surface complex at present. The resonance Raman charge-transfer process itself, however, would involve the resonance transfer of electron from metal to vacant orbitals of adsorbate and the subsequent emission of Raman photon from the vibrationally excited molecule.

We have measured the relative enhancement ratio, *R*, defined as the relative intensity of the Raman band of pyridine adsorbed on the ReO_3 nanocrystals divided by the relative intensity of corresponding band of pyridine in the liquid state. From Table 1, we see that *R* varies between 1.7 and 6.6, depending on the particle size. We observe maximum values of the enhancement ratios of the pyridine bands with the 17 nm ReO_3 nanocrystals. Comparable values of *R* for pyridine adsorbed on Ag and Au are reported in the literature.[25] The highest *R* is found in the case of the 1027 cm^{-1} (ν_{18a}, A_1) band of adsorbed pyridine. A quantitative explanation for the spectral differences (intensity and frequency) on the different metal surfaces, for example ReO_3 compared to Ag or Au, is difficult to provide at present. It is

TABLE 1: Raman Band Positions (cm^{-1}) and Relative Enhancement Ratios of Pyridine

		on 32.5 nm ReO_3		on 17 nm ReO_3		on 12 nm ReO_3	
liquid peak position (rel intens)	ν[a]	peak position (rel intens)	R[b]	peak position (rel intens)	R[b]	peak position (rel intens)	R[b]
608, A_1 (6)	6a	610 (10)	1.7	610 (15)	2.5	610 (11)	1.8
650, B_2 (8)	6b	632 (15)	2	634 (19.2)	2.4	634 (19)	2.3
991, A_1 (100)	1	962 (100)	1	962 (100)	1	962 (100)	1
1031, A_1 (69)	12	1006 (106)	1.9	1006 (182)	2.7	1007 (205)	2.9
1068, A_1 (5)	18a	1027 (20)	4	1027 (33)	6.6	1027 (29)	5.8
1214, A_1 (8)	9a	1201 (14)	1.8	1201 (26)	3.3	1201 (19)	2.4
1582, A_1 (4)	8a	1628 (6)	1.5	1628 (9)	2.3	1628 (22)	5.5

[a] ν = Wilson number. [b] R = relative enhancement ratio.

TABLE 2: Selected Raman Band Positions (cm^{-1}) and Enhancement Factors of Pyridine

		on 32.5 nm ReO_3		on 17 nm ReO_3		on 12 nm ReO_3	
liquid peak position (rel intens)	ν[a]	peak position (rel intens)	EF[b]	peak position (rel intens)	EF[b]	peak position (rel intens)	EF[b]
608, A_1 (6)	6a	610 (10)	1.90×10^5	610 (15)	2.67×10^6	610 (11)	3.05×10^6
1031, A_1 (69)	12	1006 (106)	1.43×10^4	1006 (182)	1.96×10^5	1007 (205)	2.68×10^5
1214, A_1 (8)	9a	1201 (14)	3.34×10^4	1201 (26)	4.41×10^5	1201 (19)	4.60×10^5

[a] ν = Wilson number. [b] EF = enhancement factor.

known that the vibrational spectral features of adsorbate can vary from one surface to another. Thus, the intensity of the ν_{12} band, which is the second strongest band of pyridine in liquid and gas phases, is high on Ag, but weak on Au and Cu.[25] On ReO_3, the ν_{12} band is more intense than the ν_1 band. The potential energy distribution of the ν_{12} mode appears to vary significantly for metals with different Fermi levels.

We have calculated the surface enhancement factor (EF) for pyridine molecules adsorbed on ReO_3 nanocrystals by using the following equation:[2,19]

$$\mathrm{EF} = (I_{\mathrm{SERS}}/I_{\mathrm{bulk}})(N_{\mathrm{bulk}}/N_{\mathrm{ads}})$$

where I_{SERS}, I_{bulk}, N_{bulk}, and N_{ads} represent the measured SERS intensity for adsorbed pyridine molecules on ReO_3 nanocrystals, normal Raman intensity from liquid pyridine, the number of the probe molecules under laser illumination for the bulk sample, and the number of probe molecules on the ReO_3 surface, respectively. N_{ads} is calculated from the average radius of ReO_3 nanoparticles, the surface density of the adsorbate molecule, the area of the laser spot, and surface coverage of ReO_3 nanoparticles. To calculate EF, we use the value of the monolayer surface density of pyridine[16] on Au as 4×10^{-10} mol·cm^{-2}. N_{bulk} was obtained from area of the laser spot, the penetration depth, the density of the analyte, and the molecular weight of the analyte. The value of N_{bulk} for pyridine is 2.45×10^{-13} mol. The values of EF calculated for the $\nu_{6a,}$ ν_{12}, and ν_{9a} bands of pyridine adsorbed on the 12, 17, and 32.5 nm ReO_3 nanocrystals are listed in Table 2. A similar EF for adsorbed pyridine on Ag colloids nanospheres is reported.[10] The values being around of 10^6, 10^4, and 10^2 for 5, 50, and 500 nm of Ag colloids, respectively.[10] Fleischmann et al.[7] reported EF of the order of 10^6 for pyridine on an electrochemically roughened Ag electrode. Orendorff et al.[9] have observed EF's for 4-mercaptopyridine on 31 nm Au nanoparticles and 34 nm Ag nanoparticles, which are 1.2×10^4 and 4.8×10^6, respectively. In all the cases, the EF decreases with the increase in particle size. SERS-active systems must ideally possess structures in the 5−100 nm range.[3] Likewise, the dimensions of the active structure cannot be much smaller than a lower bound. The upper bound of the SERS-active system is determined by the wavelength. For a given metal system, the SERS intensity is optimal when the particle size is small with respect to the wavelength of exciting light as long as the size is not much smaller than the electronic mean free path of the conduction electrons.[3]

TABLE 3: Raman Band Positions (cm^{-1}), Relative Enhancement Ratios, and Enhancement Factors of Pyrimidine

	on 17 nm ReO_3			
liquid peak position (rel intens)	peak position (rel intens)	R[a]	EF[b]	ν[c]
624, B_2 (6)	620 (17)	2.8	3.6×10^5	6b
675, A_1 (6)	666 (25)	4.2	5.5×10^5	6a
991, A_1 (100)	965 (100)	1	1.3×10^5	1
	986, B_1 (19)			5
1053, A_1 (14)	1010 (56)	4	5.4×10^5	(10b + 16b)FR
1075, A_1 (16)	1060 (29)	1.8	3.1×10^5	12

[a] R = relative enhancement ratio. [b] EF = enhancement factor. [c] ν = Wilson number.

The results discussed hitherto clearly demonstrate how ReO_3 nanoparticles can be effectively used to investigate SERS of pyridine. We have extended the SERS study to pyrimidine and pyrazine. Figure 3 shows the Raman spectrum of pyrimidine on the 17 nm ReO_3 nanocrystals along with that of the pure liquid. On adsorption of pyrimidine on ReO_3, we observe bands at 620 (ν_{6b}, B_2, ring in-plane deformation), 666 (ν_{6a}, A_1, ring in-plane deformation), 965 (ν_1, A_1, ring stretching), 986 (ν_5, B_1, C−H out-of-plane deformation), 1010 (Fermi resonance, A_1), and 1060 cm^{-1} (ν_{12}, A_1, ring stretching).[36] In Table 3, we show the Raman band positions of pyrimidine and the relative intensities in parentheses. Adsorbed pyrimidine bands are shifted to the lower frequencies compared to the bands of liquid pyrimidine, due to bonding between the adsorbed molecule and the ReO_3 surface. The highest frequency shifts are found in the case of 1053 (ν_{12}, ring stretching) and 991 cm^{-1} (ν_1, ring stretching) bands of pyrimidine on the ReO_3 nanocrystals. We also observe a new band at 986 cm^{-1} (ν_5, C−H out-of-plane deformation). We have enlisted the relative enhancement ratios of the adsorbed pyrimidine bands in Table 3. The value of R varies between 1.8 and 4.2. Comparable values of R for

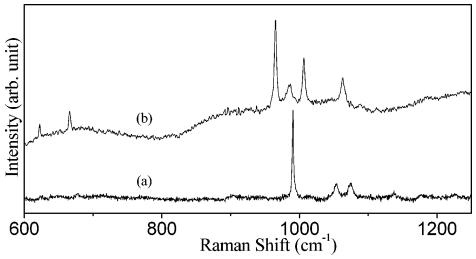

Figure 3. Raman spectra of pyrimidine: (a) in liquid state and (b) on 17 nm ReO_3.

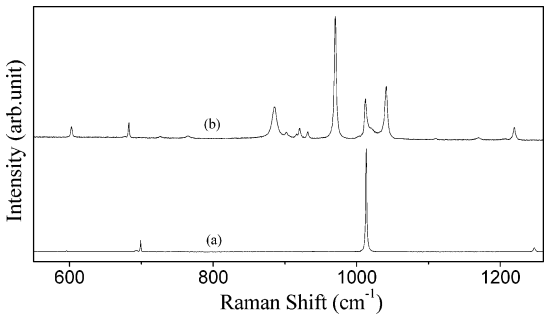

Figure 4. Raman spectra of pyrazine: (a) in liquid state and (b) on 17 nm ReO_3.

TABLE 4: Raman Band Positions in (cm^{-1}), Relative Enhancement Ratios, and Enhancement Factors of Pyrazine

	on 17 nm ReO_3			
liquid peak position (rel intens)	peak position (rel intens)	R[a]	EF[b]	ν[c]
594, A_g (1.1)	602 (8.9)	8.1	6.6×10^7	6a
693, (0.9)	677, (1.08)	1.2		
700, B_{2g} (11.7)	682 (12.5)	1.1	4.3×10^5	4
752, B_{1g} (0.8)	726 (1.5)	1.9	7.9×10^5	10a
	765, B_{3u} (2)			11
	885, (26)			
930, B_{2g} (0.6)	901 (4.8)	8	4.1×10^7	5
	920, (7.8)			
	932 (4.6)			
1015, A_g (100)	970 (100)	1	3.5×10^5	1
	1012, B_{1u} (30)			12
	1042, B_{2u} (44)			15
	1110, B_{3g} (1.1)			
	1169, B_{1u} (1.7)			18a
1243, A_g (4.5)	1219 (10)	2.3	1.9×10^6	9a
1580, A_g (1.05)	1589 (6.2)	5.9	2.3×10^6	8a

[a] R = relative enhancement ratio. [b] EF = enhancement factor. [c] ν = Wilson number.

pyrimidine adsorbed on Ag sols are reported in the literature.[12] The intensities of the A_1 type bands are generally higher, as also the values of R. The bands of the A_2 species are either absent or weak. We have estimated the enhancement factor for the Raman bands of pyrimidine using the same procedure employed for pyridine and listed them in the Table 3. The value of N_{bulk} for pyrimidine is 2.52×10^{-13} mol. Centeno et al.,[36] on the basis of their experiments and calculations, propose perpendicular orientation of pyrimidine on the Ag surface (end-on), with the surface complex having C_s symmetry. The red shifts of the band observed by us, however, seem to favor a flat-on configuration for the pyrimidine molecule.

Figure 4 shows the Raman spectra of liquid pyrazine solution and of that adsorbed on 17 nm ReO_3 nanocrystals. In Table 4, we show the Raman band positions of pyrazine and the relative intensities in parentheses. Raman bands of adsorbed pyrazine are also at lower frequencies than the bands of liquid pyrazine solution, suggesting the pyrazine molecule is likely to have a flat-on orientation on the ReO_3 surface. The highest frequency shift is in the case of the 1015 cm^{-1} (ν_1, ring breathing) band of pyrazine. Only the band at 1580 cm^{-1} (ν_{8a}, ring streching) is shifted to higher frequency. We observe new bands belonging to the B_{1u}, B_{2u}, B_{3u}, and B_{3g} species. Thus, the bands at 765 (B_{3u}), 1012 (B_{1u}) ,1042 (B_{2u}), and 1169 cm^{-1} (B_{1u}) are Raman forbidden and IR-active. The appearance of Raman forbidden bands in the spectra of the adsorbed molecule is probably due to the break down of selection rules. Dornhaus et al.[11] have shown that pyrazine adsorbed on an Ag electrode exhibits all IR-active modes in the SERS spectrum. The presence of Raman forbidden bands in the SERS spectrum of pyrazine on Ni electrodes has been observed by Huang et al.[22] Erdheim et al.[37] propose that when pyrazine is adsorbed on a metal surface, the symmetry of the molecule is lowered from D_{2h} to C_{2v} by the removal of the inversion element. This would change the Raman forbidden modes into active modes. The value of R for pyrazine varies between 1.1 and 8.1. Comparable values of R for pyrazine adsorbed on Ag sols are reported in the literature.[12] The values of R are high for bands of the A_g and B_{2g} species. We have calculated the enhancement factors for Raman bands of adsorbed pyrazine and listed them in Table 4. To calculate EF, the value of N_{bulk} is used as 2.57×10^{-13} mol.

Conclusions

We have observed SERS of aza-aromatics on nanocrystals of an oxide metal for the first time. Thus, we observe large shifts of the bands of pyridine toward the lower frequencies on adsorption of the molecules on the ReO_3 nanocrystal surface. The observed SERS effect suggests that there is bonding interaction between the metallic ReO_3 surface and the adsorbed molecules. We observe enhancement of Raman signal intensities on ReO_3 nanocrystal surfaces comparable to those on noble metals. On the basis of the spectral features, we are unable to decide on the exact geometry of the adsorbed pyridine on ReO_3 surfaces, although the red shifts of the bands are indicative of a flat-on configuration. Preliminary studies of pyrimidine and pyrazine adsorbed on ReO_3 nanocrystals also show SERS effect similar to pyridine. In the case of adsorbed pyrazine, we observe the appearance of new bands, some of which are IR-active.

References and Notes

(1) Chang, R. K.; Furtak, T. E. *Surface Enhanced Raman Scattering*; Plenum Press: New York, 1982.
(2) Tian, Z. Q.; Ren, B.; Wu, D. Y. *J. Phys. Chem. B* **2002**, *106*, 9463.
(3) Moskovits, M. *J. Raman Spectrosc.* **2005**, *36*, 485.
(4) Kneipp, K.; Kneipp, H.; Itzkan, I.; Dasari, R. R.; Feld, M. S. *Chem. Rev.* **1999**, *99*, 1957.
(5) Orendorff, C. J.; Gole, A.; Sau, T. K.; Murphy, C. J. *Anal. Chem.* **2005**, *77*, 3261.
(6) Campion, A.; Kambhampati, P. *Chem. Soc. Rev.* **1998**, *27*, 241.
(7) Fleischmann, M.; Hendra, P. J.; McQuillan, A. J. *Chem. Phys. Lett.* **1974**, *26*, 163.
(8) Lee, C.; Bae, S. J; Gong, M.; Kim, K.; Joo, S.-W. *J. Raman Spectrosc.* **2002**, *33*, 429.
(9) Orendorff, C. J.; Gearheart, L.; Jana, N. R.; Murphy, C. J. *Phys. Chem. Chem. Phys.* **2006**, *8*, 165.
(10) Kerker, M. *Pure Appl. Chem.* **1984**, *56*, 1429.
(11) Dornhaus, R.; Long, M. B.; Benner, R. E. Chang, R. K. *Surf. Sci.* **1980**, *93*, 240.
(12) Miranda, M. M.; Neto, N.; Sbrana, G. *J. Phys. Chem.* **1988**, *92*, 954.
(13) Wang, H. H.; Liu, C. Y.; Wu, S. B.; Liu, N. W.; Peng, C. Y.; Chan, T. H.; Hsu, C. F.; Wang, J. K.; Wang, Y. L. *Adv. Mater.* **2006**, *18*, 491.
(14) Michaels, A. M.; Nirmal, M.; Brus L. E. *J. Am. Chem. Soc.* **1999**, *121*, 9932.
(15) Bosnick, K. A.; Jiang, J.; Brus. L. E. *J. Phys. Chem. B* **2002**, *106*, 8096.

(16) Brolo, A. G.; Irish, D. E.; Lipkowski, J. *J. Phys. Chem. B* **1997**, *101*, 3906.
(17) Felidj, N.; Truong. S. L.; Aubard, J.; Levi, G.; Krenn, J. R.; Hohenau, A.; Leitner, A.; Aussenegg, F. R. *J. Chem. Phys.* **2004**, *120*, 7141.
(18) Yang, X.-C.; Fang, Y. *J. Phys. Chem. B* **2003**, *107*, 10100.
(19) Zhu, Z.; Zhu, T.; Liu, Z. *Nanotechnology* **2004**, *15*, 357.
(20) Ren, B.; Huang, Q. J.; Chai, W. B.; Mao, B. W.; Liu, F. M.; Tian, Z. Q. *J. Electroanal. Chem.* **1996**, *415*, 175.
(21) Gao, J. S.; Tian, Z. Q. *Spectrochim. Acta* **1997**, A 53, 1595.
(22) Huang, Q. J.; Yao, J. L.; Gu, R. A.; Tian, Z. Q. *Chem. Phys. Lett.* **1997**, *271*, 101.
(23) Cao, P. G.; Yao, J. L.; Ren, B.; Mao, B. W.; Gu;, R. A.; Tian, Z. Q. *Chem. Phys. Lett.* **2000**, *316*, 1.
(24) Wu, D. Y.; Xie, Y.; Ren, B.; Yan, J. W.; Mao, B. W.; Tian, Z. Q. *Phys. Chem. Commun.* **2001**, *18*, 1.
(25) Zuo, C.; Jagodzinski, P. W. *J. Phys. Chem. B* **2005**, *109*, 1788.
(26) Nie, S.; Emory, S. R. *Science* **1997**, *275*, 1102.
(27) Jiang, J.; Bosnik, K.; Maillard, M.; Brus, L. *J. Phys. Chem. B* **2003**, *107*, 9964.
(28) Xu, X. H.; Bjerneld, E. J.; Kall, M.; Borjesson, L. *Phys. Rev. Lett.* **1999**, *83*, 4357.
(29) Michaels, A. M.; Jiang, J.; Brus, L. *J. Phys. Chem. B* **2000**, *104*, 11965.
(30) (a) Rao, C. N. R.; Raveau, B. *Transition Metal Oxides*, 2nd ed.; Wiley-VCH: Weinheim, Germany, 1995. (b) Ferretti, A.; Rogers, D. B.; Goodenough, J. B. *J. Phys. Chem. Solids* **1965**, *26*, 2007.
(31) Biswas, K.; Rao, C. N. R. *J. Phys. Chem. B* **2006**, *110*, 842.
(32) Nechamkin, H.; Kurtz, A. N.; Hiskey, C. F. *J. Am. Chem. Soc.* **1951**, *73*, 2828.
(33) Audrieth, L. F. *Inorg. Synth.* **1950**, *3*, 187.
(34) Ishii, M.; Tanaka, T.; Akahane, T.; Tsuda, N. *J. Phys. Soc. Jpn.* **1976**, *41*, 908.
(35) Moskovits, M.; DiLella, D. P. *J. Chem. Phys*. **1980**, *73*, 6068.
(36) Centeno, S. P; Tocón, I. L.; Arenas, J. F.; Soto, J.; Otero, J. C. *J. Phys. Chem. B* **2006**, *110*, 14916.
(37) Erdheim, G. R.; Brike, R. L.; Lombardi, J. R. *Chem. Phys. Lett.* **1980**, *69*, 495.